MATERIALS CHEMISTRY
FRONTIERS

REVIEW

View Article Online
View Journal | View Issue

Cite this: *Mater. Chem. Front.*, 2023, **7**, 5731

Recent advances in electrode interface modifications in perovskite solar cells

Jiantao Wang and Hsing-Lin Wang *

Received 29th May 2023,
Accepted 14th July 2023

DOI: 10.1039/d3qm00610g

rsc.li/frontiers-materials

Perovskite solar cells (PSCs) have attracted increasing attention in the past decade due to their low cost and ease of manufacture, which make them promising candidates for next-generation photovoltaic technologies. However, the long-term stability of PSCs is still a major challenge that needs to be addressed before they can be commercialized. Interface engineering is a promising strategy to improve the performance and stability of PSCs. Here, we review the latest progress of interface modifications in PSCs, focusing on electrode interface layers. We discuss energy band alignment, carrier transport dynamics, interfacial defect passivation, and device stability in relation to electrode interface modifying materials. Finally, we discuss the challenges and opportunities of electrode interface modifications in PSCs based on recent advances.

1. Introduction

The world's transition to a net-zero carbon economy requires the development of clean energy, such as photovoltaics (PV), which can convert inexhaustible solar energy into electricity and hence largely reduce the supply of nonrenewable fossil fuels.[1] Silicon (Si) solar cells currently occupy >90% of the global PV market, due to a combination of their high efficiency, low cost, and long lifetime.[2] However, developing higher efficiency per manufacturing cost of solar cells is still essential.[3] In recent years, metal-halide perovskite semiconductors have attracted significant attention due to their excellent properties, including solution processing, tunable bandgap, broad absorption spectrum, long carrier diffusion length, and fast charge separation.[4–10] These properties enable the fabrication of perovskite solar cells (PSCs) with low cost and high power-conversion efficiency (PCE).[11–13] Since the first report of PSCs with a PCE of 3.8% in 2009, single-junction PSCs have achieved rapidly increasing efficiency to a certified 26.0% in the last decade, and perovskite-based tandem solar cells such as perovskite/Si tandems have reached 33.7%.[14] These achievements make PSCs one of the most promising candidates for the next-generation PV market.

Despite the impressive progress in PCE, the long-term stability of PSCs remains a major challenge for their practical

Department of Materials Science and Engineering, Southern University of Science and Technology, Xueyuan Avenue 1088, Shenzhen 518055, China.
E-mail: wangxl3@sustech.edu.cn

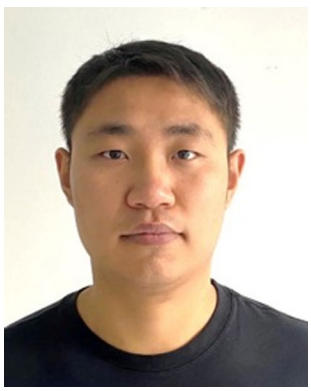

Jiantao Wang

Dr Jiantao Wang completed his PhD under the supervision of Prof. Hsing-Lin Wang in the Joint Education Program of the Southern University of Science and Technology (SUSTech) and the Hong Kong University of Science and Technology (HKUST). Currently, he is a Postdoctoral Fellow in the KPV-LAB led by Prof. Stefaan De Wolf at King Abdullah University of Science and Technology (KAUST). His research focuses on designing stable narrow- and wide-bandgap perovskite compositions and integrating them into tandem solar cells and modules.

Hsing-Lin Wang

Prof. Hsing-Lin Wang received his PhD in Chemistry from the University of South Florida in 1992. He then became a Postdoctoral Fellow at the University of Pennsylvania from 1993–1995. He came to Los Alamos National Laboratory as a Postdoctoral Fellow in 1995 and became a scientist in 1998. In 2016, he joined the Southern University of Science and Technology as a Chair Professor. His research interests include organic synthesis, processing, and applications of functional polymers, fullerene derivatives, and nanostructured materials.

application and commercialization.[15–17] The instability of PSCs is mainly attributed to the intrinsic instability of perovskite materials and the degradation of device components under environmental factors, such as moisture, oxygen, light, heat, and mechanical stress.[18–21] To improve the stability of PSCs, various strategies have been proposed, including careful design of perovskite compositions, additives, processing methods, interfacial modifications, and encapsulations.[22–31] Interface engineering is one of the most promising approaches to achieve both high performance and stability of PSCs.[32–34] This involves the modification of the interfaces between different layers in the device structure.[35,36] Interface engineering can not only optimize the energy band alignment and charge transport dynamics at the interfaces but also passivate the interfacial defects and protect the perovskite layer from external stimuli.[37–41] Among the various interfaces in PSCs, the electrode interfaces play a crucial role in determining the performance and stability of the devices. They can influence the charge extraction, recombination, and migration processes in PSCs, and thus affect the efficiency, hysteresis, and degradation of the devices.[19,42] The electrode interfaces can be modified by introducing various materials, which can act as interfacial modifiers to improve the carrier extraction efficiency, reduce the charge recombination and leakage loss, enhance the interfacial adhesion and mechanical flexibility, and prevent moisture and oxygen infiltration.[43–46]

In this review, we summarize the recent advances in electrode interface modifications in PSCs. We focus on different electrode interface modifying materials and their effects on device performance and stability. We discuss electrode interface engineering strategies for various types of PSCs. Finally, we highlight the challenges and opportunities of electrode interface modifications in PSCs based on the current state-of-the-art.

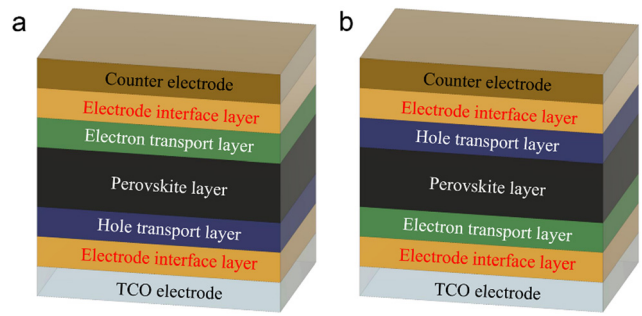

Fig. 1 Electrode interface layers in a typical perovskite solar cell with (a) p–i–n and (b) n–i–p structures, respectively.

2. The role of electrode interface layers

Reviews on interfacial engineering of PSCs typically focus on the interfaces between the perovskite layer and the electron/hole transport layers, covering several mechanisms by which interfacial engineering can improve PSCs such as defect passivation, energy band alignment, and morphological control.[37,47,48] Here, we focus on specific aspects of the electrode interface layers (EILs), which refer to the thin layers in direct contact with transparent conductive oxide (TCO) and counter electrode, as marked in red color in Fig. 1(a) and (b).[49] The EILs are optionally selected for device fabrication in terms of different types of electrodes in PSCs with p–i–n or n–i–p structures (Fig. 1). For example, when fabricating PSCs with n–i–p structure, a device without EILs has already achieved a very high PCE of 25.7%, because the widely used hole transport layer 2,2′,7,7′-tetrakis[*N*,*N*-di(4-methoxyphenyl)amino]-9,9′-spirobifluorene (Spiro-OMeTAD)/electron transport layer tin oxide (SnO_2) has matched a work function with the external gold (Au) anode/fluorine-doped tin

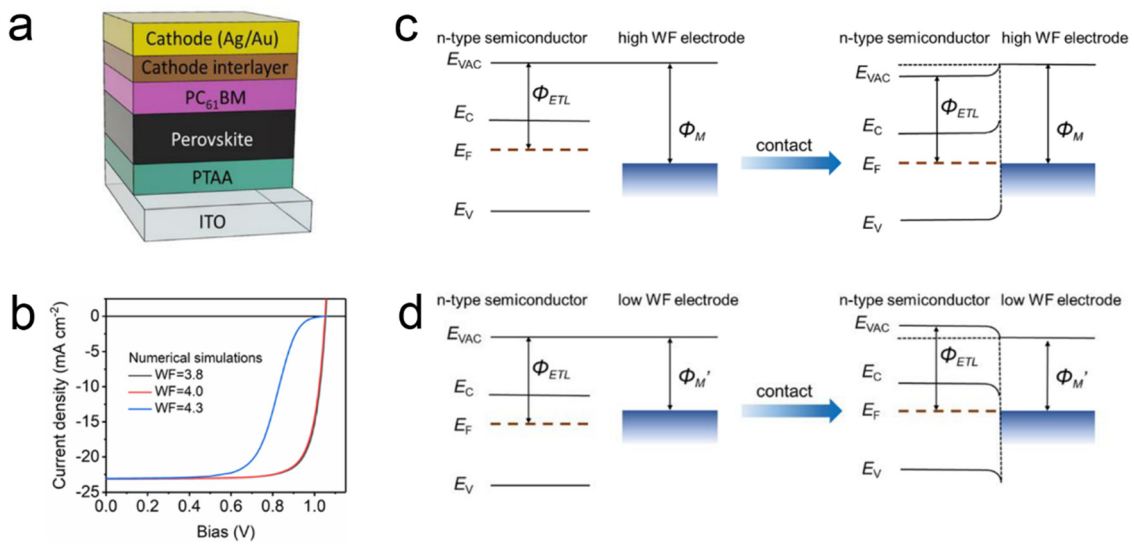

Fig. 2 (a) p–i–n device structure with cathode interlayer. (b) Numerical simulations of *J*–*V* curves based on different counter electrode work functions. Illustration of the band bending in the condition of (c) a high work function electrode and (d) a low work function electrode as the cathode. Reproduced with permission.[51] Copyright 2021, American Chemical Society Publications.

oxide (FTO) cathode.[50] However, when considering the combination of different electrodes and transporting layers for some reasons *i.e.* reducing the manufacturing cost, enhancing the device PCE and improving the operational stability, *etc.*, the problem arises with the interface energy level mismatch. This instance is more common at the interface of the electron transport layer/electrode. In some cases, the hole transport layer is allowed to contact and modify the anode directly. Hence, some of the EILs belong to the hole-transporting layer.

2.1 Tuning electrode work function

For a typical PSC with p–i–n structure as shown in Fig. 2(a), the external cathode commonly uses low-work function metals such as silver (Ag), copper (Cu), and aluminum (Al)

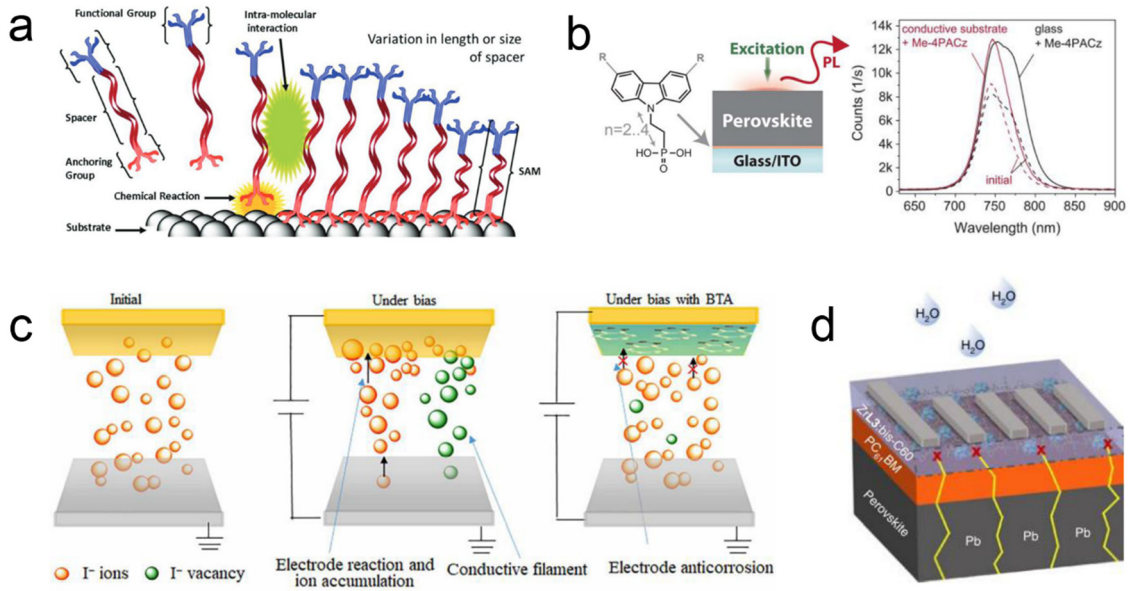

Fig. 3 (a) Schematic diagram of the mechanism of self-assembly monolayers (SAM). Reproduced with permission.[53] Copyright 2020, Wiley-VCH. (b) Photoluminescence (PL) and chemical structure of a general carbazole-based SAM, where R denotes a substitution, which is either nothing (2PACz), a methoxy group (MeO-2PACz), or a methyl group (Me-4PACz). The number 2 or 4 denotes the number of linear C atoms between the phosphonic acid anchor group and the conjugated carbazole main fragment. PL spectra before (dashed lines) and after 600 s of light-soaking (solid lines) under 1 sun illumination in air. Reproduced with permission.[52] Copyright 2020, Science Publishing Groups. (c) Electrode corrosion of perovskite-based resistive random-access memory. Reproduced with permission.[44] Copyright 2020, Science Publishing Groups. (d) Schematic of the degradation process of PSCs and the immobilization effect of the cathode interlayer on leaked Pb^{2+} ions. Reproduced with permission.[54] Copyright 2020, Nature Publishing Groups.

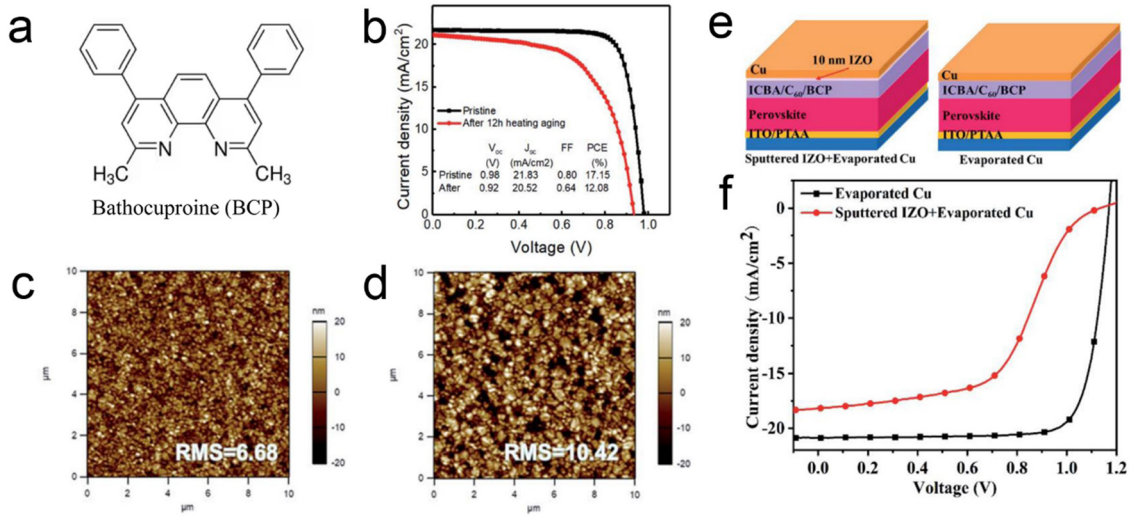

Fig. 4 (a) Molecular structure of BCP. (b) *J*–*V* curves of BCP-based devices before and after thermal aging at 85 °C for 12 h. AFM morphology of BCP films (c) before and (d) after thermal aging at 85 °C for 12 h. Reproduced with permission.[65] Copyright 2020, RSC Publications. (e) Schematics of perovskite solar cells with and without a 10 nm indium-zinc-oxide (IZO) film under the Cu electrode. (f) *J*–*V* characteristics of perovskite solar cells with Cu and IZO/Cu electrodes. Reproduced with permission.[66] Copyright 2022, RSC Publications.

to collect electrons. However, these low-work function metals are chemically reactive and environmentally unstable. To improve the counter electrode stability, Wang *et al.* try to demonstrate the use of high work function Au as the cathode.[51] Numerical simulations show that increasing the work function of the cathode would largely reduce the device fill factor (FF), as shown in Fig. 2(b). The reduced performance is due to the energy barrier generation after aligning the Fermi level of the electron transport layer with the high work function electrode (Fig. 2(c)). Therefore, introducing a cathode interlayer is necessary to eliminate the energy barrier by turning the high work function of the cathode into a low work function (Fig. 2(d)).

2.2 Enhancing carrier extraction

Directly modifying the surface work function of TCO allow the EILs to be hole/electron selective. Recently, a series of self-assembly monolayers (SAM) have been employed as anchors on the indium tin oxide (ITO), replacing the role of the hole transport layer.[52] As illustrated in Fig. 3(a), the energy level of SAM can be tailored by changing the spacer length and functional groups.[53] The SAM-modified ITO has enhanced carrier extraction capability, which can also lead to improved stability for the wide bandgap perovskite with minimized phase-separation as confirmed by photoluminescence (PL) characterization (Fig. 3(b)).[52]

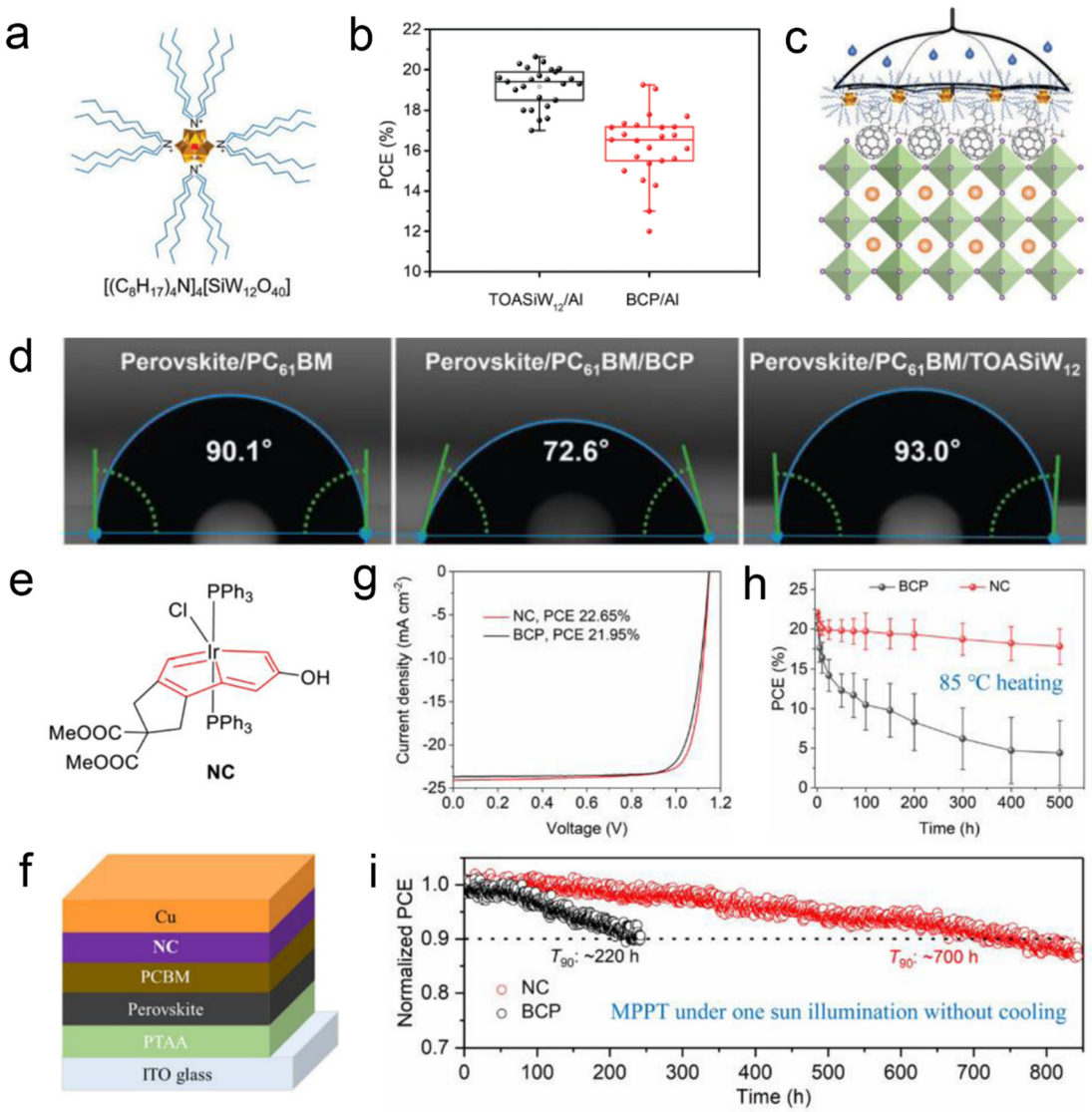

Fig. 5 (a) Molecular structure of $[(C_8H_{17})_4N]_4[SiW_{12}O_{40}]$ ($TOASiW_{12}$). (b) PCE statistics of devices based on $TOASiW_{12}$ and BCP, respectively. (c) Schematic illustration for the improvement of the $TOASiW_{12}$ layer on the water resistance of the PSCs. (d) Contact angle measurements of perovskite/$PC_{61}BM$, perovskite/$PC_{61}BM$/BCP, and perovskite/$PC_{61}BM$/$TOASiW_{12}$. Reproduced with permission.[78] Copyright 2022, Wiley. (e) Molecular structure of neutral carbolong (NC) complex. (f) Device structure with an NC cathode interlayer. (g) *J*–*V* curves, (h) thermal stability and maximum power point tracking (MPPT) of devices based on NC and BCP, respectively. Reproduced with permission.[33] Copyright 2023, RSC Publications.

2.3 Diffusion and infiltration barrier

Ion migration has been widely recognized in perovskite-based devices.[55] Studies have shown that the migrated halide ions can react with the common metal electrodes, which accelerates the device degradation.[56] Physical or chemical separating methods have been developed to hinder this process.[57] The EILs provide a barrier for internal halide diffusion. The rationally designed EILs with some special groups can also react with the electrode's inner surface, which makes the electrode unreactive to prevent diffused-halides-induced corrosion (Fig. 3(c)).[44] Likewise, some EILs can be tailored as dense and hydrophobic layers to inhibit moisture infiltration.[43] Since the moisture or water infiltration possibly leads to toxic lead leakage, which can be suppressed by modifying the EILs.[58] As shown in Fig. 3(d), Wu *et al.* added some lead-trapping materials in the EILs that can effectively minimize lead leakage.[54]

Overall, the EILs are introduced into a device basically based on the requirement of tuning the work function of electrodes. The EILs can improve the interfacial energy level alignment and enhance the carrier extraction to the electrodes. Moreover, the employment of EILs can hinder internal elements diffusion and external infiltration and thus prolong the long-term stability of PSCs.

3. Electrode interface engineering

Despite the benefits of using EILs, some of them have negative effects, such as increasing series resistance, inducing parasitic absorption, decreasing FF and short-circuit current density (J_{sc}).[59,60] It is important to optimize the selection and deposition of electrode interface modifying materials (EIMs) for PSCs to achieve a trade-off between performance and stability. In this section, we show the electrode interface engineering strategies for various types of PSCs with mainly p–i–n and n–i–p structures. We analyze the state-of-the-art results of applying EIMs to improve performance and stability.

3.1 Cathode interface modification in p–i–n PSCs

Organic small molecules and polymers are often used as EIMs because they are relatively easy to synthesize and process.[61] Organic small molecules *i.e.* bathocuproine (BCP), have been widely used as a cathode interlayer deposited before external metal electrodes in PSCs with p–i–n structure. Currently, both p–i–n structure single-junction PSCs and all-perovskite tandem solar cells with the highest PCEs use the thermal-evaporated BCP as the cathode interlayer because it effectively lowers the carrier recombination at the cathode interface.[11,62,63] However, this organic BCP layer leads to a rapid loss of device efficiency

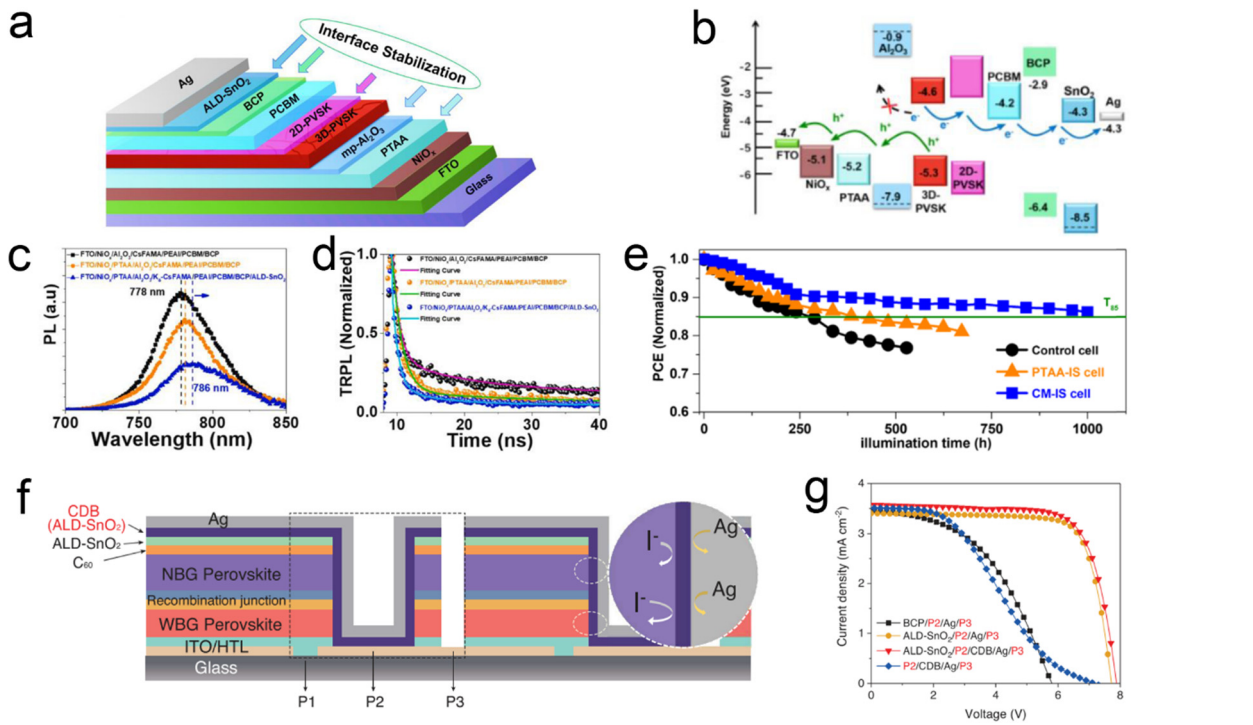

Fig. 6 (a) Conceptual mechanism with interface stabilization for long-term stable PSCs and (b) corresponding energy band diagram. (c) PL and (d) time-resolved PL (TRPL) of three films FTO/NiO_x/Al_2O_3/CsFAMA-perovskite/PEAI/PCBM/BCP (dark), FTO/NiO_x/PTAA/Al_2O_3/CsFAMA-perovskite/PEAI/PCBM/BCP (orange) and FTO/NiO_x/PTAA/Al_2O_3/KCsFAMA-perovskite/PEAI/PCBM/BCP/ALD-SnO_2 (blue). (e) Operational-stability of three devices FTO/NiO_x/Al_2O_3/CsFAMA-perovskite/PEAI/PCBM/BCP/Ag (dark), FTO/NiOx/PTAA/Al_2O_3/CsFAMA-perovskite/PEAI/PCBM/BCP/Ag (orange) and FTO/NiOx/PTAA/Al_2O_3/KCsFAMA-perovskite/PEAI/PCBM/BCP/ALD-SnO_2/Ag (blue). Reproduced with permission.[83] Copyright 2021, Elsevier B.V. Publications. (f) Schematic diagram of the structure of the series-connected all-perovskite tandem module with conformal diffusion barrier (CDB) to prevent ion diffusion. (g) *J*–*V* curves of different module configurations. Reproduced with permission.[85] Copyright 2022, Science Publishing Groups.

when tracking the stability (Fig. 4(b)), due to the crystallization of the thermally evaporated BCP layer under thermal stress, which can be observed from the morphological change before and after thermal aging under 85 °C for 12 h (Fig. 4(c) and (d)).[64,65] In addition, the BCP layer is easy to cause peel-off damage and reduces device performance when using sputtered TCO as the counter electrode (Fig. 4(e) and (f)), which have shown potential for bifacial photovoltaics and perovskite/Si tandem devices.[66–70]

Table 1 Representative molecules with passivating groups decorating between the anode and the perovskite

Passivating group	Molecular structure	Device efficiency (%)	Ref.
$-NH_3^+$	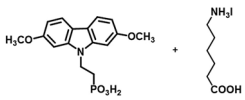	23.59	86
$-OCH_3$	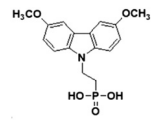	21.2	87
–S	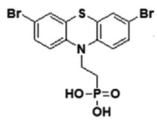	22.37	88
–Se	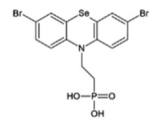	22.73	89
–P–O(H)	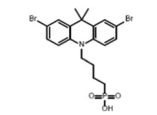	25.86	90
–CN	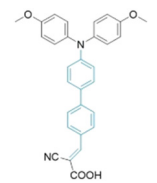	22.53	91

To replace BCP, multiple EIMs such as organic small molecules, polymers, organic–inorganic hybrid compounds, and inorganic metal oxides have been developed and shown enhancement in both the efficiency and the stability for PSCs.[71–77] Organic–inorganic hybrid EIMs with the advantages of both the structure tunability of organic molecules and the stability of inorganic materials have the potential to overcome the instability of the cathode interface. Yu *et al.* reported a surfactant encapsulated polyoxometalate complex $[(C_8H_{17})_4N]_4[SiW_{12}O_{40}]$ ($TOASiW_{12}$) (Fig. 5(a)), which can form a stable cathode interface by reacting with cathode Al.[78] The PSCs with $TOASiW_{12}O_{40}$ achieved a PCE of 20.64%, higher than BCP-based devices (Fig. 5(b)). Moreover, $TOASiW_{12}$ can effectively block moisture permeation as it has abundant alkyl chains to improve the hydrophobicity of the device (Fig. 5(c)) as confirmed by water contact angle tests (Fig. 5(d)). Wang *et al.* reported an organic–inorganic Carbolong complex used as a cathode interlayer in Cu-based PSCs (Fig. 5(e) and (f)). A neutral carbolong complex (NC) can tune the alignment of the interfacial energy level and improve the PCE to 22.65% (Fig. 5(g)).[33] The NC molecule has superior thermal properties that can facilitate the duration of a device under 85 °C heating and one-sun illuminated maximum power point tracking (MPPT) (Fig. 5(h) and (i)).

Inorganic metal oxides SnO_x have also been widely used to modify the cathode interface in p–i–n PSCs.[79–81] SnO_x have deep highest occupied molecular orbitals (HOMOs), strong hole blocking capacity, high electron mobility, and good stability.[82]

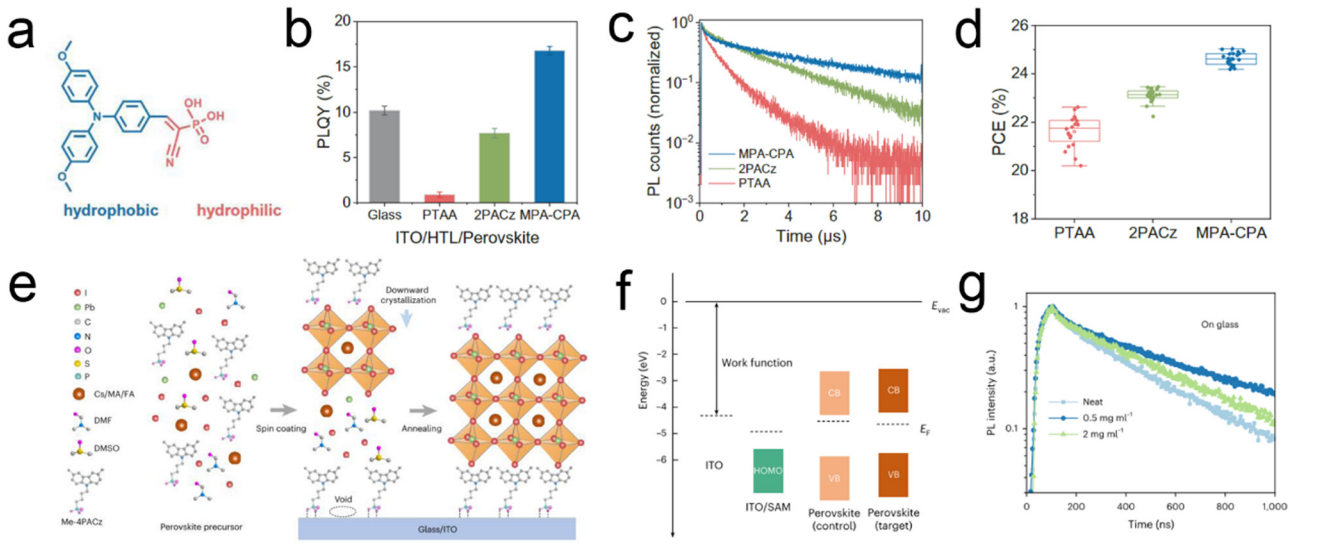

Fig. 7 (a) Molecular structure of the amphiphilic MPA-CPA molecule. (b) PL quantum yield and (c) PL decays of perovskite films on different substrates. (d) The statistics of PCE values for devices based on different HTLs. Reproduced with permission.[62] Copyright 2023, Science Publishing Groups. (e) Illustration of SAM formation and the perovskite crystallization process. (f) Energy-level diagram. (g) TRPL of perovskite films with different concentrations of Me-4PACz on glass substrates. Reproduced with permission.[13] Copyright 2022, Nature Publishing Groups.

Wang *et al.* reported SnO_x by atomic layer deposition (ALD) as a barrier layer to prevent degrading the perovskite layer from moisture and oxygen as well as halogen diffusion (Fig. 6(a)).[83] The SnO_x cathode interlayer has a matched energy level for electron transfer (Fig. 6(b)), thus enabling efficient charge separation and suppression of interfacial non-radiative recombination (Fig. 6(c) and (d)). As a result, the device with ALD SnO_x maintained 85% of the initial PCE for 1000 h under 1 sun illumination tracking. Furthermore, the ALD SnO_x technique has been mitigated to bifacial and tandem devices because the dense layer can bear the deposition of sputtered ITO and solution processing that the solvents are incompatible with the bottom layers.[84] Xiao *et al.* introduced an electrically conductive conformal diffusion barrier (CDB) consisting of ALD SnO_x between interconnecting sub-cells to improve the PCE and stability of all-perovskite tandem solar modules.[85] As presented in Fig. 6(f), the CDB layer served as both a vertical electron extractor and a lateral diffusion barrier. It also prevented direct contact between the metal electrode and the conductive poly(3,4-ethylenedioxythiophene) polystyrene sulfonate (PEDOT: PSS) in the recombination layer, which could otherwise lower the shunt resistance (Fig. 6(g)).

3.2 Anode interface modification in p–i–n PSCs

SAM of organic small molecules that can modify the TCO anode has been employed in the highest efficiency p–i–n PSCs and perovskite-based tandem solar cells.[11,62] Such organic small molecules have functions as hole-extracting layers, which can also contact the perovskite layer directly and passivate interfacial defects, depending on their chemical structure and groups.[86] We have listed the reported representative passivating agents in Table 1 according to their molecular functional groups. Recently, Zhang *et al.* reported a SAM molecule (2-(4-(bis(4-methoxyphenyl)amino)phenyl)-1-cyan vinyl)phosphonic acid (MPA-CPA) (Fig. 7(a)) with amphiphilic groups that enables efficient hole transport and the growth of high-quality perovskite films with minimized defects at the buried interface.[62] The perovskite films deposited on MPA-CPA displayed a PL quantum yield of 17%, much higher than on glass, PTAA, and 2PACz (Fig. 7(b)). The perovskite on MPA-CPA also presented the best electronic quality and suppressed nonradiative recombination as demonstrated by the time-resolved PL (TRPL) in Fig. 7(c). Thus, the device PCE could be improved to 25.4%, which is the highest efficiency in p–i–n PSCs (Fig. 7(d)). The SAM molecules can also be mixed with the perovskite precursor and co-deposited by one-step solution processing.[13] As illustrated in Fig. 7(e), the SAM molecule Me-4PACz binds to the TCO surface generating a loosely packed SAM during coating the precursor solution, and a denser and more robust SAM forms when annealing the wet perovskite film. The resulting films show elevated work function of ITO after washed-off examination and less n-type perovskite as compared to the control film without co-deposition (Fig. 7(f)). The presence of Me-4PACz reduces surface non-radiative recombination as measured by TRPL (Fig. 7(g)). The co-deposition method tackles the critical wetting issue encountered when processing perovskite onto hydrophobic SAMs and simplifies manufacturability.

3.3 Cathode interface modification in n–i–p PSCs

For a n–i–p structure device as shown in Fig. 8(a), the electron transport layer of low-temperature solution-processed [6,6]-phenyl-C_{61}-butyric acid methyl ester (PCBM) can be deposited between ITO and perovskite. However, the lowest unoccupied molecular orbital (LUMO) of n-type semiconductor PCBM has a large energy gap with the ITO electrode as shown in Fig. 8(b), which would lead to a large energy loss, reducing the open-circuit voltage (V_{oc}) and FF.[92] Introducing a polymer interlayer poly[(9,9-bis(3′-(*N*,*N*-dimethylamino) propyl)-2,7-fluorene)-*alt*-2,7-(9,9-dioctylfluorene)] (PFN) can effectively reduce the work function of ITO and improve the device performance from

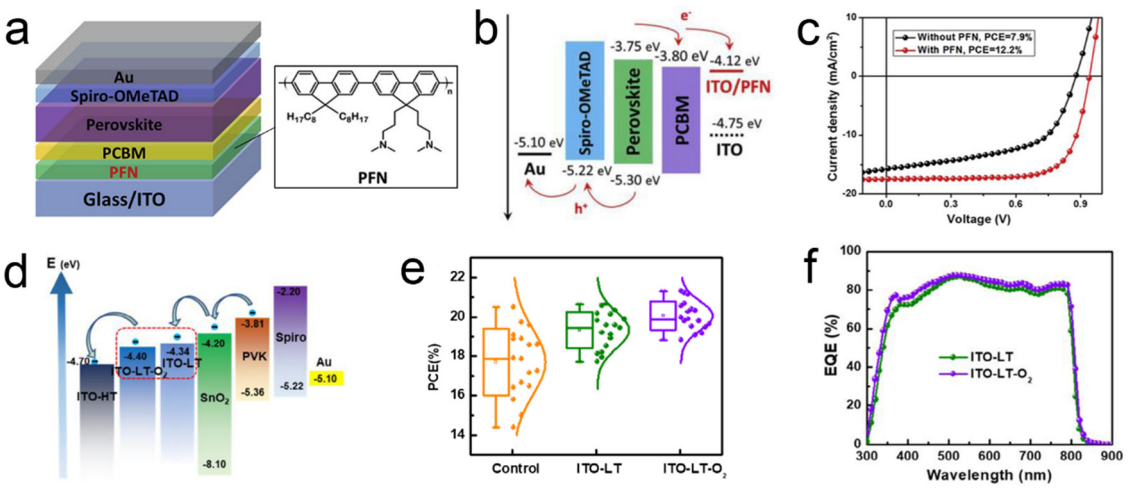

Fig. 8 (a) n–i–p device structure with a cathode interlayer PFN. (b) Energy level alignment and (c) *J*–*V* curves of devices with and without cathode interlayer modified electrode. Reproduced with permission.[92] Copyright 2017, Elsevier B.V. Publications. (d) Energy level alignment, (e) PCE statistics and (f) external quantum efficiency (EQE) of n–i–p solar cells with corresponding low-temperature processed ITO (LT-ITO) interlayer. Reproduced with permission.[93] Copyright 2023, Wiley.

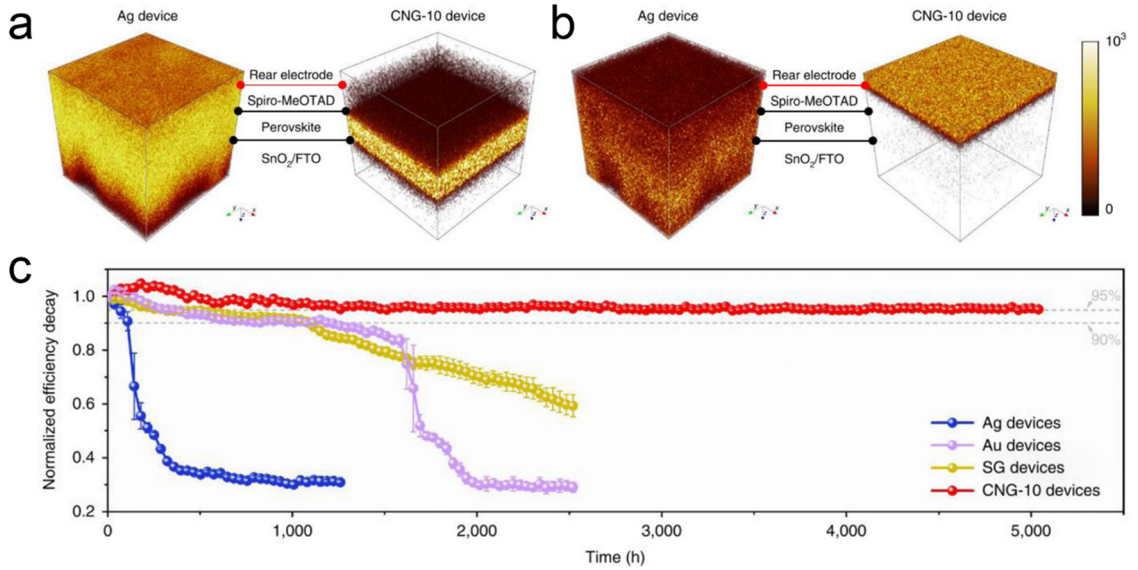

Fig. 9 (a) The spatial distribution of I^- in the aged Ag and CNG devices. (b) The spatial distribution of Ag^- and Cu^- in the aged Ag and CNG devices. (c) The operational stability of the encapsulated Ag, Au, sprayed graphene (SG), and CNG-10 devices at the MPP under one sun illumination. Reproduced with permission.[38] Copyright 2022, Nature Publishing Groups.

7.9% to 12.2% (Fig. 8(c)). To eliminate the interface energy mismatch between ITO and SnO_x ETL, Chen *et al.* reported a low-temperature-processed ITO (ITO-LT) cathode buffer layer.[93] Interfacial charge transfer could be enhanced by introducing a 3 nm sputtered ITO cathode buffer layer with an appropriate energy alignment and effective defect suppression of oxygen vacancies in it, leading to a PCE of 21.13% in PSCs (Fig. 8(d) and (e)). The defect control by oxygen vacancies management could improve device J_{sc} confirmed from the external quantum efficiency (EQE) enhancement (Fig. 8(f)).

3.4 Anode interface modification in n–i–p PSCs

The anode interlayer can act as a barrier to enhance the stability of n–i–p PSCs. Carbon materials such as graphene and fullerene derivatives have attracted considerable attention as promising EIMs for PSCs due to their excellent electrical, optical, and mechanical properties, as well as their abundance and environmental friendliness.[94] Carbon materials can be incorporated into PSCs in various forms, such as thin films or composites.[95] Lin *et al.* reported *in situ* grown graphene to modify the copper–nickel (Cu–Ni) alloy anode enabling long-term stable operation of PSCs.[38] The Cu–Ni alloy and graphene (CNG) electrode can effectively block the interdiffusion of halides and electrode metals (Fig. 9(a) and (b)), which make the device to operate for 5000 h and keep the PCE to 95% (Fig. 9(c)).

4. Conclusions and outlook

The electrode interfacial layer (EIL) is vital in perovskite solar cells (PSCs) as it can tune the electrode work function and improve interfacial energy level match, enhance carrier transport, and form a barrier to external infiltration and halide diffusion. Tremendous efforts have been made to develop electrode interface modifying materials (EIMs) to improve the efficiency and stability of PSCs. The electrode interface engineering strategy has been applied in various types of PSCs including p–i–n and n–i–p structure and perovskite-based tandem devices by rationally designing the EIMs and introducing them as the EILs.

However, there are some remaining challenges in modifying the electrode interface in PSCs. Basically, the processing of EIMs should enable scalability. Most of the EIMs are processed by lab-scale spin-coating technique. The methods to fabricate large-area and uniform films based on the current EIMs lack further demonstration. Second, the EIMs must have compatibility with the processing of other layers. The EIMs on the TCO side should be insoluble in the solution of the top layers and avoid dissolving the bottom layers when deposited on the counter electrode side by solution-processing. More efforts should be invested in future research regarding developing novel EIMs, optimizing the interfacial properties and structures, integrating with other stability improvement methods, and exploring new applications and markets for PSCs.

Conflicts of interest

The authors have no conflicts of interest to declare.

Acknowledgements

The authors acknowledge the funding support from the Key-Area Research and Development Program of Guang Dong Province (2019B010941001) and Shenzhen Fundamental Research Scheme-General Program (JCYJ20220818100217037).

References

1 N. M. Haegel, P. Verlinden, M. Victoria, P. Altermatt, H. Atwater, T. Barnes, C. Breyer, C. Case, S. D. Wolf, C. Deline, M. Dharmrin, B. Dimmler, M. Gloeckler, J. C. Goldschmidt, B. Hallam, S. Haussener, B. Holder, U. Jaeger, A. Jaeger-Waldau, I. Kaizuka, H. Kikusato, B. Kroposki, S. Kurtz, K. Matsubara, S. Nowak, K. Ogimoto, C. Peter, I. M. Peters, S. Philipps, M. Powalla, U. Rau, T. Reindl, M. Roumpani, K. Sakurai, C. Schorn, P. Schossig, R. Schlatmann, R. Sinton, A. Slaoui, B. L. Smith, P. Schneidewind, B. Stanbery, M. Topic, W. Tumas, J. Vasi, M. Vetter, E. Weber, A. W. Weeber, A. Weidlich, D. Weiss and A. W. Bett, Photovoltaics at multi-terawatt scale: Waiting is not an option, *Science*, 2023, **380**, 39–42.

2 L. Meng, J. You and Y. Yang, Addressing the stability issue of perovskite solar cells for commercial applications, *Nat. Commun.*, 2018, **9**, 5265.

3 M. A. Green, A. Ho-Baillie and H. J. Snaith, The emergence of perovskite solar cells, *Nat. Photonics*, 2014, **8**, 506–514.

4 D. W. deQuilettes, S. M. Vorpahl, S. D. Stranks, H. Nagaoka, G. E. Eperon, M. E. Ziffer, H. J. Snaith and D. S. Ginger, Impact of microstructure on local carrier lifetime in perovskite solar cells, *Science*, 2015, **348**, 683–686.

5 S. D. Stranks, G. E. Eperon, G. Grancini, C. Menelaou, M. J. P. Alcocer, T. Leijtens, L. M. Herz, A. Petrozza and H. J. Snaith, Electron-Hole Diffusion Lengths Exceeding 1 Micrometer in an Organometal Trihalide Perovskite Absorber, *Science*, 2015, **342**, 341–344.

6 M. M. Lee, J. Teuscher, T. Miyasaka, T. N. Murakami and H. J. Snaith, Efficient Hybrid Solar Cells Based on Meso-Superstructured Organometal Halide Perovskites, *Science*, 2012, **338**, 643–647.

7 J. Xu, C. C. Boyd, Z. J. Yu, A. F. Palmstrom, D. J. Witter, B. W. Larson, R. M. France, J. Werner, S. P. Harvey, E. J. Wolf, W. Weigand, S. Manzoor, M. F. A. M. v Hest, J. J. Berry, J. M. Luther, Z. C. Holman and M. D. McGehee, Triple-halide wide–band gap perovskites with suppressed phase segregation for efficient tandems, *Science*, 2020, **367**, 1097–1104.

8 G. E. Eperon, T. Leijtens, K. A. Bush, R. Prasanna, T. Green, J. T.-W. Wang, D. P. McMeekin, G. Volonakis, R. L. Milot, R. May, A. Palmstrom, D. J. Slotcavage, R. A. Belisle, J. B. Patel, E. S. Parrott, R. J. Sutton, W. Ma, F. Moghadam, B. Conings, A. Babayigit, H.-G. Boyen, S. Bent, F. Giustino, L. M. Herz, M. B. Johnston, M. D. McGehee and H. J. Snaith, Perovskite-perovskite tandem photovoltaics with optimized band gaps, *Science*, 2016, **354**, 861–865.

9 W. S. Yang, J. H. Noh, N. J. Jeon, Y. C. Kim, S. Ryu, J. Seo and S. I. Seok, High-performance photovoltaic perovskite layers fabricated through intramolecular exchange, *Science*, 2015, **348**, 1234–1237.

10 J. Wu, H. Cha, T. Du, Y. Dong, W. Xu, C. T. Lin and J. R. Durrant, A Comparison of Charge Carrier Dynamics in Organic and Perovskite Solar Cells, *Adv. Mater.*, 2021, e2101833, DOI: **10.1002/adma.202101833**.

11 R. He, W. Wang, Z. Yi, F. Lang, C. Chen, J. Luo, J. Zhu, J. Thiesbrummel, S. Shah, K. Wei, Y. Luo, C. Wang, H. Lai, H. Huang, J. Zhou, B. Zou, X. Yin, S. Ren, X. Hao, L. Wu, J. Zhang, J. Zhang, M. Stolterfoht, F. Fu, W. Tang and D. Zhao, All-perovskite tandem 1 cm(2) cells with improved interface quality, *Nature*, 2023, **618**, 80–86, DOI: **10.1038/s41586-023-05992-y**.

12 Q. Jiang, J. Tong, Y. Xian, R. A. Kerner, S. P. Dunfield, C. Xiao, R. A. Scheidt, D. Kuciauskas, X. Wang, M. P. Hautzinger, R. Tirawat, M. C. Beard, D. P. Fenning, J. J. Berry, B. W. Larson, Y. Yan and K. Zhu, Surface reaction for efficient and stable inverted perovskite solar cells, *Nature*, 2022, **611**, 278–283.

13 X. Zheng, Z. Li, Y. Zhang, M. Chen, T. Liu, C. Xiao, D. Gao, J. B. Patel, D. Kuciauskas, A. Magomedov, R. A. Scheidt, X. Wang, S. P. Harvey, Z. Dai, C. Zhang, D. Morales, H. Pruett, B. M. Wieliczka, A. R. Kirmani, N. P. Padture, K. R. Graham, Y. Yan, M. K. Nazeeruddin, M. D. McGehee, Z. Zhu and J. M. Luther, Co-deposition of hole-selective contact and absorber for improving the processability of perovskite solar cells, *Nat. Energy*, 2023, **8**, 462–472, DOI: **10.1038/s41560-023-01227-6**.

14 NREL best research-cell efficiencies chart, **https://www.nrel.gov/pv/assets/pdfs/best-research-cell-efficiencies.pdf**, 2023.

15 Z. Li, B. Li, X. Wu, S. A. Sheppard, S. Zhang, D. Gao, N. J. Long and Z. Zhu, Organometallic functionalized interfaces for highly efficient inverted perovskite solar cells, *Science*, 2022, **376**, 416–420.

16 X. Li, W. Zhang, X. Guo, C. Lu, J. Wei and J. Fang, Constructing heterojunctions by surface sulfidation for efficient inverted perovskite solar cells, *Science*, 2022, **375**, 434–437.

17 J.-P. Correa-Baena, M. Saliba, T. Buonassisi, M. Grätzel, A. Abate, W. Tress and A. Hagfeldt, Promises and challenges of perovskite solar cells, *Science*, 2017, **358**, 739–744.

18 S. Chen, X. Dai, S. Xu, H. Jiao, L. Zhao and J. Huang, Stabilizing perovskite-substrate interfaces for high-performance perovskite modules, *Science*, 2021, **373**, 902–907.

19 Y. Zhao, T. Heumueller, J. Zhang, J. Luo, O. Kasian, S. Langner, C. Kupfer, B. Liu, Y. Zhong, J. Elia, A. Osvet, J. Wu, C. Liu, Z. Wan, C. Jia, N. Li, J. Hauch and C. J. Brabec, A bilayer conducting polymer structure for planar perovskite solar cells with over 1400 hours operational stability at elevated temperatures, *Nat. Energy*, 2021, **7**, 144–152.

20 K. Domanski, E. A. Alharbi, A. Hagfeldt, M. Gratzel and W. Tress, Systematic investigation of the impact of operation conditions on the degradation behaviour of perovskite solar cells, *Nat. Energy*, 2018, **3**, 61–67.

21 S. Bitton and N. Tessler, Perovskite ionics – elucidating degradation mechanisms in perovskite solar cells *via* device modelling and iodine chemistry, *Energy Environ. Sci.*, 2023, **16**, 2621–2628, DOI: **10.1039/d3ee00881a**.

22 S. Wang, C. Wu, H. Yao, L. Ding and F. Hao, The nonhalides in perovskite solar cells, *Mater. Chem. Front.*, 2023, **7**, 789–805.

23 D.-K. Lee and N.-G. Park, Additive engineering for highly efficient and stable perovskite solar cells, *Appl. Phys. Rev.*, 2023, **10**, 0113081.

24 J. Wang, M. A. Uddin, B. Chen, X. Ying, Z. Ni, Y. Zhou, M. Li, M. Wang, Z. Yu and J. Huang, Enhancing Photostability of Sn–Pb Perovskite Solar Cells by an Alkylammonium Pseudo-Halogen Additive, *Adv. Energy Mater.*, 2023, **13**, 2204115, DOI: 10.1002/aenm.202204115.
25 J. Wang, F. Meng, R. Li, S. Chen, X. Huang, J. Xu, X. Lin, R. Chen, H. Wu and H.-L. Wang, Boosting Efficiency and Stability of Planar Inverted $(FAPbI_3)_x(MAPbBr_3)_{1-x}$ Solar Cells *via* $FAPbI_3$ and $MAPbBr_3$ Crystal Powders, *Sol. RRL*, 2020, **4**, 2000091.
26 N. J. Jeon, J. H. Noh, Y. C. Kim, W. S. Yang, S. Ryu and S. I. Seok, Solvent engineering for high-performance inorganic-organic hybrid perovskite solar cells, *Nat. Mater.*, 2014, **13**, 897–903.
27 T. Wang, J. Yang, Q. Cao, X. Pu, Y. Li, H. Chen, J. Zhao, Y. Zhang, X. Chen and X. Li, Room temperature nondestructive encapsulation *via* self-crosslinked fluorosilicone polymer enables damp heat-stable sustainable perovskite solar cells, *Nat. Commun.*, 2023, **14**, 1342.
28 X. Qi, J. Wang, F. Tan, C. Dong, K. Liu, X. Li, L. Zhang, H. Wu, H. L. Wang, S. Qu, Z. Wang and Z. Wang, Quantum Dot Interface-Mediated $CsPbIBr_2$ Film Growth and Passivation for Efficient Carbon-Based Solar Cells, *ACS Appl. Mater. Interfaces*, 2021, **13**, 55349–55357.
29 J. Wang, J. Xu, Z. Li, X. Lin, C. Yu, H. Wu and H.-L. Wang, Front-Contact Passivation of PIN $MAPbI_3$ Solar Cells with Superior Device Performances, *ACS Appl. Energy Mater.*, 2020, **3**, 6344–6351.
30 H. Li, J. Zhou, L. Tan, M. Li, C. Jiang, S. Wang, X. Zhao, Y. Liu, Y. Zhang, Y. Ye, W. Tress and C. Yi, Sequential vacuum-evaporated perovskite solar cells with more than 24% efficiency, *Sci. Adv.*, 2022, **8**, eabo7422.
31 L. Shi, M. P. Bucknall, T. L. Young, M. Zhang, L. Hu, J. Bing, D. S. Lee, J. Kim, T. Wu, N. Takamure, D. R. McKenzie, S. Huang, M. A. Green and A. W. Y. Ho-Baillie, Gas chromatography–mass spectrometry analyses of encapsulated stable perovskite solar cells, *Science*, 2020, **368**, eaba2412.
32 Y. Li, H. Xie, E. L. Lim, A. Hagfeldt and D. Bi, Recent Progress of Critical Interface Engineering for Highly Efficient and Stable Perovskite Solar Cells, *Adv. Energy Mater.*, 2021, **12**, 2102730.
33 J. Wang, J. Li, H. Liu, Z. Lu, H. Xia and H.-L. Wang, Interface engineering using a neutral carbolong complex for efficient and stable p–i–n perovskite solar cells, *J. Mater. Chem. C*, 2023, **11**, 2480–2483.
34 F. Li and A. K. Y. Jen, Interface Engineering in Solution-Processed Thin-Film Solar Cells, *Acc. Mater. Res.*, 2022, **3**, 272–282.
35 J. Li, J. Wang, Y. Zhou, C. Yu, H. Liu, X. Qi, R. Li, Y. Hua, Y. Yu, R. Chen, D. Chen, L. Mao, H. Xia and H.-L. Wang, Boosting the performance and stability of inverted perovskite solar cells by using a carbolong derivative to modulate the cathode interface, *Mater. Chem. Front.*, 2022, **6**, 2211–2218.
36 X. T. Meng, X. Cui, M. Rager, S. G. Zhang, Z. W. Wang, J. Yu, Y. W. Harn, Z. T. Kang, B. K. Wagner, Y. Liu, C. Yu, J. S. Qiu and Z. Q. Lin, Cascade charge transfer enabled by incorporating edge-enriched graphene nanoribbons for mesostructured perovskite solar cells with enhanced performance, *Nano Energy*, 2018, **52**, 123–133.
37 W. Yu, X. Sun, M. Xiao, T. Hou, X. Liu, B. Zheng, H. Yu, M. Zhang, Y. Huang and X. Hao, Recent advances on interface engineering of perovskite solar cells, *Nano Res.*, 2021, **15**, 85–103.
38 X. Lin, H. Su, S. He, Y. Song, Y. Wang, Z. Qin, Y. Wu, X. Yang, Q. Han, J. Fang, Y. Zhang, H. Segawa, M. Grätzel and L. Han, In situ growth of graphene on both sides of a Cu–Ni alloy electrode for perovskite solar cells with improved stability, *Nat. Energy*, 2022, **7**, 520–527.
39 Y. Ma, X. Meng, K. Li, L. Zhang, Y. Du, X. Cai and J. Qiu, Scrutinizing Synergy and Active Site of Nitrogen and Selenium Dual-Doped Porous Carbon for Efficient Triiodide Reduction, *ACS Catal.*, 2023, **13**, 1290–1298.
40 X. Zhao, X. Meng, H. Zou, Z. Wang, Y. Du, Y. Shao, J. Qi and J. Qiu, Topographic Manipulation of Graphene Oxide by Polyaniline Nanocone Arrays Enables High-Performance Solar-Driven Water Evaporation, *Adv. Funct. Mater.*, 2022, **33**, 2209207.
41 X. Meng, C. Yu, X. Song, J. Iocozzia, J. Hong, M. Rager, H. Jin, S. Wang, L. Huang, J. Qiu and Z. Lin, Scrutinizing Defects and Defect Density of Selenium-Doped Graphene for High-Efficiency Triiodide Reduction in Dye-Sensitized Solar Cells, *Angew. Chem., Int. Ed.*, 2018, **57**, 4682–4686.
42 M. Ghasemi, B. Guo, K. Darabi, T. Wang, K. Wang, C. W. Huang, B. M. Lefler, L. Taussig, M. Chauhan, G. Baucom, T. Kim, E. D. Gomez, J. M. Atkin, S. Priya and A. Amassian, A multiscale ion diffusion framework sheds light on the diffusion-stability-hysteresis nexus in metal halide perovskites, *Nat. Mater.*, 2023, **22**, 329–337.
43 N. Arora, M. I. Dar, A. Hinderhofer, N. Pellet, F. Schreiber, S. M. Zakeeruddin and M. Grätzel, Perovskite solar cells with CuSCN hole extraction layers yield stabilized efficiencies greater than 20%, *Science*, 2017, **358**, 768–771.
44 X. Li, S. Fu, W. Z. S. Ke, W. Song and J. Fang, Chemical anticorrosion strategy for stable inverted perovskite solar cells, *Sci. Adv.*, 2020, **6**, eabd1580.
45 P. Caprioglio, J. A. Smith, R. D. J. Oliver, A. Dasgupta, S. Choudhary, M. D. Farrar, A. J. Ramadan, Y. H. Lin, M. G. Christoforo, J. M. Ball, J. Diekmann, J. Thiesbrummel, K. A. Zaininger, X. Shen, M. B. Johnston, D. Neher, M. Stolterfoht and H. J. Snaith, Open-circuit and short-circuit loss management in wide-gap perovskite p–i–n solar cells, *Nat. Commun.*, 2023, **14**, 932.
46 H. Zou, X. Meng, X. Zhao and J. Qiu, Hofmeister Effect-Enhanced Hydration Chemistry of Hydrogel for High-Efficiency Solar-Driven Interfacial Desalination, *Adv. Mater.*, 2023, **35**, e2207262.
47 Z. Guo, Z. Wu, Y. Chen, S. Wang and W. Huang, Recent advances in the interfacial engineering of organic–inorganic hybrid perovskite solar cells: a materials perspective, *J. Mater. Chem. C*, 2022, **10**, 13611–13645.
48 D. Y. Heo, W. J. Jang and S. Y. Kim, Recent review of interfacial engineering for perovskite solar cells: effect of

functional groups on the stability and efficiency, *Mater. Today Chem.*, 2022, **26**, 101224.

49 B. Lyu, L. Yang, Y. Luo, X. Zhang and J. Zhang, Counter electrodes for perovskite solar cells: materials, interfaces and device stability, *J. Mater. Chem. C*, 2022, **10**, 10775–10798.

50 J. Park, J. Kim, H. S. Yun, M. J. Paik, E. Noh, H. J. Mun, M. G. Kim, T. J. Shin and S. I. Seok, Controlled growth of perovskite layers with volatile alkylammonium chlorides, *Nature*, 2023, **616**, 724–730.

51 J. Wang, J. Li, Y. Zhou, C. Yu, Y. Hua, Y. Yu, R. Li, X. Lin, R. Chen, H. Wu, H. Xia and H. L. Wang, Tuning an Electrode Work Function Using Organometallic Complexes in Inverted Perovskite Solar Cells, *J. Am. Chem. Soc.*, 2021, **143**, 7759–7768.

52 A. Al-Ashouri, E. Köhnen, B. Li, A. Magomedov, H. Hempel, P. Caprioglio, J. A. Márquez, A. B. M. Vilches, E. Kasparavicius, J. A. Smith, N. Phung, D. Menzel, M. Grischek, L. Kegelmann, D. Skroblin, C. Gollwitzer, T. Malinauskas, M. Jošt, G. Matič, B. Rech, R. Schlatmann, M. Topič, L. Korte, A. Abate, B. Stannowski, D. Neher, M. Stolterfoht, T. Unold, V. Getautis and S. Albrecht, Monolithic perovskite/silicon tandem solar cell with >29% efficiency by enhanced hole extraction, *Science*, 2020, **370**, 1300–1309.

53 F. Ali, C. Roldán-Carmona, M. Sohail and M. K. Nazeeruddin, Applications of Self-Assembled Monolayers for Perovskite Solar Cells Interface Engineering to Address Efficiency and Stability, *Adv. Energy Mater.*, 2020, **10**, 2002989.

54 S. Wu, Z. Li, M. Q. Li, Y. Diao, F. Lin, T. Liu, J. Zhang, P. Tieu, W. Gao, F. Qi, X. Pan, Z. Xu, Z. Zhu and A. K. Jen, 2D metal–organic framework for stable perovskite solar cells with minimized lead leakage, *Nat. Nanotechnol.*, 2020, **15**, 934–940.

55 Y. Zhao, I. Yavuz, M. Wang, M. H. Weber, M. Xu, J. H. Lee, S. Tan, T. Huang, D. Meng, R. Wang, J. Xue, S. J. Lee, S. H. Bae, A. Zhang, S. G. Choi, Y. Yin, J. Liu, T. H. Han, Y. Shi, H. Ma, W. Yang, Q. Xing, Y. Zhou, P. Shi, S. Wang, E. Zhang, J. Bian, X. Pan, N. G. Park, J. W. Lee and Y. Yang, Suppressing ion migration in metal halide perovskite *via* interstitial doping with a trace amount of multivalent cations, *Nat. Mater.*, 2022, **21**, 1396–1402.

56 H. Lee and C. Lee, Analysis of Ion-Diffusion-Induced Interface Degradation in Inverted Perovskite Solar Cells *via* Restoration of the Ag Electrode, *Adv. Energy Mater.*, 2018, **8**, 1702197.

57 E. Bi, H. Chen, F. Xie, Y. Wu, W. Chen, Y. Su, A. Islam, M. Gratzel, X. Yang and L. Han, Diffusion engineering of ions and charge carriers for stable efficient perovskite solar cells, *Nat. Commun.*, 2017, **8**, 15330.

58 X. Jin, Y. Yang, T. Zhao, X. Wu, B. Liu, M. Han, W. Chen, T. Chen, J.-S. Hu and Y. Jiang, Mitigating Potential Lead Leakage Risk of Perovskite Solar Cells by Device Architecture Engineering from Exterior to Interior, *ACS Energy Lett.*, 2022, **7**, 3618–3636.

59 L. Xu, J. Liu, F. Toniolo, M. De Bastiani, M. Babics, W. Yan, F. Xu, J. Kang, T. Allen, A. Razzaq, E. Aydin and S. De, Wolf, Monolithic Perovskite/Silicon Tandem Photovoltaics with Minimized Cell-to-Module Losses by Refractive-Index Engineering, *ACS Energy Lett.*, 2022, **7**, 2370–2372.

60 J. Peng, D. Walter, Y. Ren, M. Tebyetekerwa, Y. Wu, T. Duong, Q. Lin, J. Li, T. Lu, M. A. Mahmud, O. L. C. Lem, S. Zhao, W. Liu, Y. Liu, H. Shen, L. Li, F. Kremer, H. T. Nguyen, D.-Y. Choi, K. J. Weber, K. R. Catchpole and T. P. White, Nanoscale localized contacts for high fill factors in polymer-passivated perovskite solar cells, *Science*, 2021, **371**, 390–395.

61 J. Wang, Z. Yu, D. D. Astridge, Z. Ni, L. Zhao, B. Chen, M. Wang, Y. Zhou, G. Yang, X. Dai, A. Sellinger and J. Huang, Carbazole-Based Hole Transport Polymer for Methylammonium-Free Tin–Lead Perovskite Solar Cells with Enhanced Efficiency and Stability, *ACS Energy Lett.*, 2022, **7**, 3353–3361.

62 S. Zhang, F. Ye, X. Wang, R. Chen, H. Zhang, L. Zhan, X. Jiang, Y. Li, X. Ji, S. Liu, M. Yu, F. Yu, Y. Zhang, R. Wu, Z. Liu, Z. Ning, D. Neher, L. Han, Y. Lin, H. Tian, W. Chen, M. Stolterfoht, L. Zhang, W.-H. Zhu and Y. Wu, Minimizing buried interfacial defects for efficientinverted perovskite solar cells, *Science*, 2023, **380**, 404–409.

63 J. Y. Jeng, Y. F. Chiang, M. H. Lee, S. R. Peng, T. F. Guo, P. Chen and T. C. Wen, $CH_3NH_3PbI_3$ perovskite/fullerene planar-heterojunction hybrid solar cells, *Adv. Mater.*, 2013, **25**, 3727–3732.

64 Y. Deng, S. Xu, S. Chen, X. Xiao, J. Zhao and J. Huang, Defect compensation in formamidinium–caesium perovskites for highly efficient solar mini-modules with improved photostability, *Nat. Energy*, 2021, **6**, 633–641.

65 X. Zheng, T. Jiang, L. Bai, X. Chen, Z. Chen, X. Xu, D. Song, X. Xu, B. Li and Y. M. Yang, Enhanced thermal stability of inverted perovskite solar cells by interface modification and additive strategy, *RSC Adv.*, 2020, **10**, 18400–18406.

66 K. Liu, B. Chen, Z. J. Yu, Y. Wu, Z. Huang, X. Jia, C. Li, D. Spronk, Z. Wang, Z. Wang, S. Qu, Z. C. Holman and J. Huang, Reducing sputter induced stress and damage for efficient perovskite/silicon tandem solar cells, *J. Mater. Chem. A*, 2022, **10**, 1343–1349.

67 B. Chen, Z. Yu, A. Onno, Z. Yu, S. Chen, J. Wang, Z. C. Holman and J. Huang, Bifacial all-perovskite tandem solar cells, *Sci. Adv.*, 2022, **8**, eadd0377.

68 M. De Bastiani, A. J. Mirabelli, Y. Hou, F. Gota, E. Aydin, T. G. Allen, J. Troughton, A. S. Subbiah, F. H. Isikgor, J. Liu, L. Xu, B. Chen, E. Van Kerschaver, D. Baran, B. Fraboni, M. F. Salvador, U. W. Paetzold, E. H. Sargent and S. De Wolf, Efficient bifacial monolithic perovskite/silicon tandem solar cells *via* bandgap engineering, *Nat. Energy*, 2021, **6**, 167–175.

69 M. De Bastiani, A. S. Subbiah, M. Babics, E. Ugur, L. Xu, J. Liu, T. G. Allen, E. Aydin and S. De Wolf, Bifacial perovskite/silicon tandem solar cells, *Joule*, 2022, **6**, 1431–1445.

70 H. Gu, C. Fei, G. Yang, B. Chen, M. A. Uddin, H. Zhang, Z. Ni, H. Jiao, W. Xu, Z. Yan and J. Huang, Design optimization of bifacial perovskite minimodules for improved efficiency and stability, *Nat. Energy*, 2023, **8**, 675–684, DOI: **10.1038/s41560-023-01254-3**.

71 A. Sharma, S. Singh, X. Song, D. Rosas Villalva, J. Troughton, D. Corzo, L. Toppare, G. Gunbas, B. C. Schroeder and D. Baran, A Nonionic Alcohol Soluble Polymer Cathode Interlayer Enables Efficient Organic and Perovskite Solar Cells, *Chem. Mater.*, 2021, **33**, 8602–8611.
72 W. Chen, L. Xu, X. Feng, J. Jie and Z. He, Metal Acetylacetonate Series in Interface Engineering for Full Low-Temperature-Processed, High-Performance, and Stable Planar Perovskite Solar Cells with Conversion Efficiency over 16% on 1 cm(2) Scale, *Adv. Mater.*, 2017, **29**, 1603923.
73 Z. Hu, J. S. Miao, T. T. Li, M. Liu, I. Murtaza and H. Meng, Reduced interface losses in inverted perovskite solar cells by using a simple dual-functional phenanthroline derivative, *Nano Energy*, 2018, **43**, 72–80.
74 N. Liu, J. Xiong, G. Wang, Z. He, J. Dai, Y. Zhang, Y. Huang, Z. Zhang, D. Wang, S. Li, B. Liu, X. Deng, H. Zhang and J. Zhang, Overcoming the PCBM/Ag Interface Issues in Inverted Perovskite Solar Cells by Rhodamine-Functionalized Dodecahydro-Closo-Dodecaborate Derivate Interlayer, *Adv. Funct. Mater.*, 2023, **33**, 2300396, DOI: **10.1002/adfm.202300396**.
75 T. Wu, D. Wang, X. Jiang, F. Guo, T. Ye, S. Gao and Y. Zhang, Polar side-chain tuning of perylene diimide and fluorene-based cathode interfacial material for high-performance inverted perovskite solar cells, *Mater. Chem. Front.*, 2023, **7**, 483–489.
76 D. Wang, C. Kang, T. Ye, D. He, S. Jin, X. Zhang, X. Sun and Y. Zhang, A novel perylene diimide-based ionene polymer and its mixed cathode interlayer strategy for efficient and stable inverted perovskite solar cells, *J. Energy Chem.*, 2023, **82**, 334–342.
77 P. Cai, L. Ding, Z. Chen, D. Wang, H. Peng, C. Yuan, C. Hu, L. Sun, Y. N. Luponosov, F. Huang and Q. Xue, Tetrabutylammonium Bromide Functionalized $Ti_3C_2T_x$ MXene as Versatile Cathode Buffer Layer for Efficient and Stable Inverted Perovskite Solar Cells, *Adv. Funct. Mater.*, 2023, **33**, 2300113, DOI: **10.1002/adfm.202300113**.
78 C. Yu, Y. Hu, J. Yang, J. Huang, B. Li, L. Wu and F. Li, Efficient and Stable Inverted Perovskite Solar Cells with $TOASiW_{12}$-Modified Al as a Cathode, *Adv. Funct. Mater.*, 2022, **33**, 2209290.
79 Z. Yu, J. Wang, B. Chen, M. A. Uddin, Z. Ni, G. Yang and J. Huang, Solution-Processed Ternary Tin(II) Alloy as Hole-Transport Layer of Sn–Pb Perovskite Solar Cells for Enhanced Efficiency and Stability, *Adv. Mater.*, 2022, **34**, e2205769.
80 R. Prasanna, T. Leijtens, S. P. Dunfield, J. A. Raiford, E. J. Wolf, S. A. Swifter, J. Werner, G. E. Eperon, C. de Paula, A. F. Palmstrom, C. C. Boyd, M. F. A. M. van Hest, S. F. Bent, G. Teeter, J. J. Berry and M. D. McGehee, Design of low bandgap tin-lead halide perovskite solar cells to achieve thermal, atmospheric and operational stability, *Nat. Energy*, 2019, **4**, 939–947.
81 X. P. Zheng, Y. Hou, C. X. Bao, J. Yin, F. L. Yuan, Z. R. Huang, K. P. Song, J. K. Liu, J. Troughton, N. Gasparini, C. Zhou, Y. B. Lin, D. J. Xue, B. Chen, A. K. Johnston, N. Wei, M. N. Hedhili, M. Y. Wei, A. Y. Alsalloum, P. Maity, B. Turedi, C. Yang, D. Baran, T. D. Anthopoulos, Y. Han, Z. H. Lu, O. F. Mohammed, F. Gao, E. H. Sargent and O. M. Bakr, Managing grains and interfaces *via* ligand anchoring enables 22.3%-efficiency inverted perovskite solar cells, *Nat. Energy*, 2020, **5**, 131–140.
82 Q. Jiang, X. Zhang and J. You, SnO(2): A Wonderful Electron Transport Layer for Perovskite Solar Cells, *Small*, 2018, e1801154, DOI: **10.1002/smll.201801154**.
83 Y. Wang, H. Ju, T. Mahmoudi, C. Liu, C. Zhang, S. Wu, Y. Yang, Z. Wang, J. Hu, Y. Cao, F. Guo, Y.-B. Hahn and Y. Mai, Cation-size mismatch and interface stabilization for efficient NiOx-based inverted perovskite solar cells with 21.9% efficiency, *Nano Energy*, 2021, **88**, 106285.
84 B. Abdollahi Nejand, D. B. Ritzer, H. Hu, F. Schackmar, S. Moghadamzadeh, T. Feeney, R. Singh, F. Laufer, R. Schmager, R. Azmi, M. Kaiser, T. Abzieher, S. Gharibzadeh, E. Ahlswede, U. Lemmer, B. S. Richards and U. W. Paetzold, Scalable two-terminal all-perovskite tandem solar modules with a 19.1% efficiency, *Nat. Energy*, 2022, **7**, 620–630.
85 K. Xiao, Y.-H. Lin, M. Zhang, R. D. J. Oliver, X. Wang, Z. Liu, X. Luo, J. Li, D. Lai, H. Luo, R. Lin, J. Xu, Y. Hou, H. J. Snaith and H. Tan, Scalable processing for realizing 21.7%-efficient all-perovskite tandem solar modules, *Science*, 2022, **376**, 762–767.
86 X. Deng, F. Qi, F. Li, S. Wu, F. R. Lin, Z. Zhang, Z. Guan, Z. Yang, C. S. Lee and A. K. Jen, Co-assembled Monolayers as Hole-Selective Contact for High-Performance Inverted Perovskite Solar Cells with Optimized Recombination Loss and Long-Term Stability, *Angew. Chem., Int. Ed.*, 2022, **61**, e202203088.
87 A. Al-Ashouri, A. Magomedov, M. Ross, M. Jost, M. Talaikis, G. Chistiakova, T. Bertram, J. A. Marquez, E. Kohnen, E. Kasparavicius, S. Levcenco, L. Gil-Escrig, C. J. Hages, R. Schlatmann, B. Rech, T. Malinauskas, T. Unold, C. A. Kaufmann, L. Korte, G. Niaura, V. Getautis and S. Albrecht, Conformal monolayer contacts with lossless interfaces for perovskite single junction and monolithic tandem solar cells, *Energy Environ. Sci.*, 2019, **12**, 3356–3369.
88 A. Ullah, K. H. Park, H. D. Nguyen, Y. Siddique, S. F. A. Shah, H. Tran, S. Park, S. I. Lee, K. K. Lee, C. H. Han, K. Kim, S. Ahn, I. Jeong, Y. S. Park and S. Hong, Novel Phenothiazine-Based Self-Assembled Monolayer as a Hole Selective Contact for Highly Efficient and Stable p–i–n Perovskite Solar Cells, *Adv. Energy Mater.*, 2021, **12**, 2103175.
89 A. Ullah, K. H. Park, Y. Lee, S. Park, A. B. Faheem, H. D. Nguyen, Y. Siddique, K. K. Lee, Y. Jo, C. H. Han, S. Ahn, I. Jeong, S. Cho, B. Kim, Y. S. Park and S. Hong, Versatile Hole Selective Molecules Containing a Series of Heteroatoms as Self-Assembled Monolayers for Efficient p–i–n Perovskite and Organic Solar Cells, *Adv. Funct. Mater.*, 2022, **32**, 2208793.
90 Q. Tan, Z. Li, G. Luo, X. Zhang, B. Che, G. Chen, H. Gao, D. He, G. Ma, J. Wang, J. Xiu, H. Yi, T. Chen and Z. He, Inverted perovskite solar cells using dimethylacridine-based dopants, *Nature*, 2023, DOI: **10.1038/s41586-023-06207-0**.

91 S. Zhang, R. Wu, C. Mu, Y. Wang, L. Han, Y. Wu and W.-H. Zhu, Conjugated Self-Assembled Monolayer as Stable Hole-Selective Contact for Inverted Perovskite Solar Cells, *ACS Mater. Lett.*, 2022, 1976–1983, DOI: **10.1021/acsmaterialslett.2c00799**.
92 X. Xie, G. Liu, C. Xu, S. Li, Z. Liu and E.-C. Lee, Tuning the work function of indium-tin-oxide electrodes for low-temperature-processed, titanium-oxide-free perovskite solar cells, *Org. Electron.*, 2017, **44**, 120–125.
93 B. Chen, Y. Chen, Z. Zhu, G. Hou, Q. Huang, Y. Zhao and X. Zhang, Cathode Buffer Layer for Energy-Level Matching and Interface Passivation, *Sol. RRL*, 2022, **7**, 2200865.
94 M. Hadadian, J. H. Smatt and J. P. Correa-Baena, The role of carbon-based materials in enhancing the stability of perovskite solar cells, *Energy Environ. Sci.*, 2020, **13**, 1377–1407.
95 V. Ferguson, S. R. P. Silva and W. Zhang, Carbon Materials in Perovskite Solar Cells: Prospects and Future Challenges, *Energy Environ. Mater.*, 2019, **2**, 107–118.